Carbohydrate Polymers 241 (2020) 116358

Contents lists available at ScienceDirect

Carbohydrate Polymers

journal homepage: www.elsevier.com/locate/carbpol

Inducing inflammatory response in RAW264.7 and NK-92 cells by an arabinogalactan isolated from *Ferula gummosa* via NF-κB and MAPK signaling pathways

Mehdi Tabarsa[a,*], Elham Hashem Dabaghian[a], SangGuan You[b,*], Khamphone Yelithao[b], Subramanian Palanisamy[b], Narayanasamy Marimuthu Prabhu[c], Changsheng Li[b]

[a] Department of Seafood Processing, Faculty of Marine Sciences, Tarbiat Modares University, P.O. Box 46414-356, Nur, Iran
[b] Department of Marine Food Science and Technology, Gangneung-Wonju National University, Gangneung, Gangwon 25457, South Korea
[c] Disease Control and Prevention Lab, Department of Animal Health and Management, Alagappa University, Karaikudi, 630 003 Tamil Nadu, India

ARTICLE INFO

Keywords:
Arabinogalactan
Stimulation
Macrophages
Natural killer cells
Signaling pathways

ABSTRACT

The polysaccharide isolated from *F. gummosa* (FGP) was found homogenous with a weight average molecular weight (M_w) of 50.0 × 10^3 g/mol and radius of gyration (R_g) of 105.3 nm. The FGP was an arabinogalactan with a backbone formed of →6)-β-Gal*p*-1→ residues having random branching points at C-3 extended with either β-Gal*p*-(1→3)-β-Gal*p*-(1→ or α-Ara*f*-(1→ side chain residues. FGP exhibited proliferative effect on RAW264.7 cells and induced macrophages to exert proinflammatory response releasing NO and up-regulating the transcription of cytokines including TNF-α, IL-1β, IL-6 and IL-12. The FGP induced NK-92 cells to up-regulate the expressions of TNF-α, IFN-γ, granzyme-B, perforin, NKG2D and FasL. The presence of p-NF- κB, p-ERK, p-JNK and p-p38 in RAW264.7 and NK-92 cells indicated their activation through NF-κB and MAPKs signaling pathways. These findings suggested that polysaccharides from *F. gummosa* are potent in boosting immune system and thus may be considered for further studies of biomedical applications.

1. Introduction

Plant non-starch polysaccharides are gaining importance in food and biomedical sectors as a means to modify physical properties of different products, maintain normal intestinal function and introduce novel promising therapeutic benefits in an economically viable and environmentally friendly manner. This group of structurally diverse polysaccharides serves as storage and cell wall structure polymers and are located in seeds, fruits, flowers and leaves of higher plants as well as their resins exuding for protective purposes in response to injury (Liu, Willför, & Xu, 2015; Singh, Singh, & Arya, 2018). Apart from their great hydrophilic nature that makes polysaccharide exploitations exceedingly favorable, the complexity in molecular nature and heterogeneity in molecular size have granted these biomacromolecules the chemical capacity to positively meddle in a broad spectrum of biological processes (Liu et al., 2015). However, these structural peculiarities of polysaccharides have also imposed some challenging restrictions, such as high viscosity, low solubility, poor purity and the lack of understanding of structure-activity relationships, on their industrial utilizations.

As stated above, the therapeutic functions of polysaccharides are immensely diverse spanning from a wide range of chronic diseases such as cancer (Feng, Ji, Dong, Yu, & Liu, 2019), diabetes (Xiao et al., 2019) and obesity (Luo et al., 2019) to infectious diseases such as HIV/AIDS (Muschin et al., 2016), influenza (Zhao et al., 2019) and hepatitis B (Liang et al., 2019). Presently, immunostimulatory polysaccharides are a newly and rapidly growing class of biologically active compounds with paramount importance in protecting human body against bacterial and viral diseases or applying immunotherapy in diseases such as AIDS and cancer (Tripathi, Tripathi, Kashyap, & Singh, 2007). As one of the top causes of mortality worldwide, cancer encompasses a series of medical conditions characterized by deregulated and rapidly cell division with the potential to metastasize to different organs where their chemotherapy treatment could result in disabling side effects especially immunosuppression (Khan, Date, Chawda, & Patel, 2019). On the contrary to conventional chemotherapeutic agents, polysaccharides not only exhibit selective cytotoxicity and induce apoptosis on malignant cells, they are also capable of restoring the dynamic balance between the cancer cells and the immune system and eventually exert antitumor effects (Bao, Yuan, Wang, Liu, & Lan, 2013). In addition, numerous

* Corresponding authors.
E-mail addresses: m.tabarsa@modares.ac.ir (M. Tabarsa), umyousg@gwnu.ac.kr (S. You).

https://doi.org/10.1016/j.carbpol.2020.116358
Received 11 August 2019; Received in revised form 20 April 2020; Accepted 20 April 2020
Available online 26 April 2020
0144-8617/

studies have been exclusively dedicated to immunostimulatory effects of polysaccharides and results suggested their efficacy in producing inflammatory response both within the innate immunity components including macrophages, dendritic cells and natural killer cells and acquired immunity components including T and B lymphocytes (Canton, Neculai, & Grinstein, 2013; Song & Lee, 2012).

The genus *Ferula* constitutes more than 130 species with wide distribution across the world from Mediterranean areas to Central Asia and Iran (Salehi, Naghavi, & Bahmankar, 2019). The historical background of using *Ferula gummosa* in traditional medicine dates back to 3000 years ago as a remedy for internal diseases, pain relief and antiseptic for the wounds (Salehi et al., 2019). Accordingly, the findings of the modern pharmaceutical era have also showcased the invaluable health-promoting benefits of *Ferula* metabolites in prevention and treatment of virus infections, cancer, diabetes and peptic ulcer (Soltani et al., 2018; Zhou et al., 2017). Although *F. gummosa* is abundantly available and its resin contains a large amount of polysaccharide, no reports have been documented on the structural analysis and immunomodulatory effects of their polysaccharides. The purpose of this study, therefore, was to specify the structural and molecular characteristics of water-soluble polysaccharides obtained from *F. gummosa* and to determine immunostimulatory activities.

2. Materials and methods

2.1. Sample and reagents

Sample of *F. gummosa* was obtained from a local market of Nur, Mazandaran, Iran. The raw material was soaked in cold water and air dried at 60 °C. Then, it was milled using a blender, sieved (< 0.5) and stored at − 20 °C in a plastic bag until polysaccharide extraction. DEAE Sepharose Fast Flow gel was purchased from GE Healthcare Bio-Science AB (17-0709-01; Uppsala, Sweden). Fetal bovine serum (FBS), RPMI-1640 and MEM mediums used in cell culture were purchased from Lonza (Walkersville, MD, USA). All other reagents and chemicals used in this study were of analytical grade.

2.2. Polysaccharide extraction and fractionation

Initially, 20 g of sample powder was defatted and de-pigmented with 200 mL of 80 % ethanol at ambient temperature (22 ± 2 °C) under constant mechanical stirring overnight to remove low molecular weight compounds and pigments. The supernatant was discarded after centrifugation at 6080*g* for 10 min at 10 °C. This procedure repeated twice to ensure maximum removal of unwanted compounds. Afterwards, the residual parts were rinsed with acetone for several times and dried at room temperature in a fume hood. The pre-treated biomass was extracted twice with 400 mL of distilled water and the process carried out at 65 °C with stirring for 2 h. The mixture was centrifuged at 6080*g* for 10 min at 10 °C and the supernatants were combined and concentrated by evaporation at 60 °C under reduced pressure. Ethanol (99 %) was added to the concentrated supernatant to obtain a final concentration of 70 % ethanol. The polysaccharides were precipitated and dehydrated by consecutive washing steps with 99 % ethanol and a final wash with acetone. Isolated polysaccharide was designated as FGP and kept at ambient temperature to dry. The FGP was fractionated using a DEAE Sepharose Fast Flow column. For sample preparation, initially 250 mg of FGP was solubilized in 10 mL of distilled water at 65 °C for 15 min and then filtered using a 3.0 μm filter. The polysaccharide solution was loaded onto the column, eluting with distilled water and a stepwise NaCl gradient (0.5–2.0 M). The phenol-sulfuric acid assay was employed to test the eluents in which carbohydrate-positive fractions were collected, dialyzed and lyophilized (Dubois, Gilles, Hamilton, Rebers, & Smith, 1956).

2.3. Chemical composition analysis

The amount of neutral sugars in the isolated polysaccharide was measured by the phenol-sulfuric acid assay using D-glucose as a standard (Dubois et al., 1956). The protein content was estimated by the Lowry method using the DC protein assay kit (Bio-Rad, USA) (Lowry, Rosebrough, Farr, & Randall, 1951). The sulfamate/m-hydroxydiphenyl assay using glucuronic acid as a standard was employed to determine the uronic acid content (Filisetti-Cozzi & Carpita, 1991).

2.4. Determination of monosaccharides

The polysaccharide (2 mg) was hydrolyzed with 4 M TFA (trifluoroacetic acid) at 100 °C for 6 h in a sealed glass tube. The TFA was evaporated with a dry flow of nitrogen. Then, the hydrolyzed molecules were reduced with $NaBD_4$ and acetylated by acetic anhydride. The last resulting derivatives were injected into a gas chromatography system (GC) system (6890 N/MSD 5973, Agilent Technologies, Santa Clara, CA) equipped with HP-5MS capillary column (30 m × 0.25 mm × 0.25 μm) (Agilent Technologies, Santa Clara, CA).

2.5. Glycosidic linkage analysis

The Ciucanu and Kerek method (1984) was employed to determine the glycosidic linkages of the polysaccharide. Initially, the lyophilized polysaccharide (3 mg) was dissolved in 0.5 mL DMSO (dimethyl sulfoxide) under nitrogen stream. After the addition of NaOH (20 mg) and keeping the mixture for 15 min, methyl iodide (CH_3I, 0.3 mL) was added into the solution and methylation was continued for 45 min. Then, acid hydrolysis was performed on the methylated derivatives using 4 M TFA (0.5 mL) at 100 °C for 6 h. The hydrolyzed product was reduced using distilled water with $NaBD_4$ (5 mg) and acetylation was performed using acetic anhydride (0.5 mL) at 100 °C. The partially methylated alditol acetates (PMAAs) were injected into a gas chromatograph-mass spectrometer (GC–MS) (6890 N/MSD 5973, Agilent Technologies, Santa Clara, CA) equipped with HP-5MS capillary column (30 m × 0.25 mm × 0.25 μm) (Agilent Technologies, Santa Clara, CA). The carrier gas was Helium which was used at a constant flow rate of 1.2 mL/min (Bahramzadeh et al., 2019). The temperature program of the oven was as follows: from 160 to 210 °C for 10 min and then to 240 °C for 10 min. The temperature gradient was 5 °C/min and the inlet temperature was kept constant at 250 °C. The mass range was set to measure between 35 and 450 *m/z*.

2.6. NMR spectroscopy

A cycle of dissolution and drying process of polysaccharide was carried out in D_2O for two times to fully exchange H_2O with D_2O. Finally, the polysaccharide (20 mg) was dissolved in D_2O (0.5 mL) at 50 °C before NMR analysis. The NMR spectra were recorded on a JEOL ECA-600 spectrometer (JEOL, Akishima, Japan), equipped with 5 mm multinuclear auto-turning TH tunable probe. The base frequency was 150 MHz for ^{13}C and 600 MHz for ^{1}H and 2D-NMR tests were carried out using the pulse programs supplied by the manufacturer.

2.7. Determination of molecular properties

The polysaccharide was solubilized in distilled water (2 mg/mL) and heated for 30 s in a microwave bomb and filtered through a cellulose acetate membrane unit (3.0 μm pore size; Whatman International). Filtered samples (20 μL) were loaded into a high performance size exclusion chromatography column (TSK G5000 PW, 7.5 × 600 mm; Toso Biosep, Montgomeryville, PA, USA) linked to a UV detector (Waters, 2487), multi-angle laser light scattering (HELEOS; Wyatt Technology Corp, Santa Barbara, CA, USA) and refractive index detection (Waters, 2414) system (HPSEC-UV-MALLS-RI). The mobile

phase consisting of an aqueous solution of 0.15 M $NaNO_3$ and 0.02 % NaN_3 was used at a flow rate of 0.4 mL/min. ASTRA 5.3 software (Wyatt Technology Corp.) was employed to calculate the weight average molecular weight (M_w) and radius of gyration (R_g).

2.8. RAW264.7 macrophage proliferation and nitric oxide production assays

The immunostimulatory activity of the polysaccharide was determined based on the nitric oxide (NO) released by macrophages into the culture supernatants and the nitrite concentration was measured as an indicator of immunoenhancing activity of polysaccharides using the Griess reagent (Green et al., 1982). RAW264.7 cells were cultured in an RPMI-1640 medium consisting of 10 % FBS and plated in a 96-well microplate (1×10^4 cells/well, 100-μL volume; ATCC). Polysaccharides (100 μL) in different concentrations (50, 100 and 200 μg/mL) were incubated with cells in triplicate. The cell cultures were kept in humidified atmosphere containing 5% CO_2 at 37 °C for 18 h after which supernatants were separated and mixed with equal amount of Griess reagent. The amount of nitrite produced by macrophages was quantified using $NaNO_2$ (1–200 μM in culture medium) as reference. Then, the WST-1 solution (20 μL) was added into the wells and the mixture was further incubated at 37 °C for 4 h. The optical density was measured at 450 nm using a microplate reader (EL-8000; BioTek Instruments, Winooski, VT, USA). The absorbance (A) was translated into a macrophage proliferation ratio, (%) = $A_t/A_c \times 100$, where A_t and A_c are the absorbance of the test group and control group, respectively. Control group was cells cultured in polysaccharide-free RPMI-1640 medium consisting of 10 % FBS.

2.9. Reverse transcription-polymerase chain reaction (rt-PCR)

RAW264.7 cells (1×10^5 cells/well) were incubated with polysaccharides (50, 100 and 200 μg/mL) added into an RPMI-1640 medium containing 10 % FBS for 18 h at 37 °C. The NK-92 cells (7.5×10^5 cells/well) were cultured for 24 h at 37 °C in an MEM medium containing 10 % FBS, 10 % horse serum, 0.2 mM inositol, 0.02 mM folic acid, 0.1 mM β-mercaptoethanol and various concentrations of polysaccharides (50, 100 and 200 μg/mL). The extraction of total RNA from RAW264.7 and NK-92 cells was performed according to the manufacturer´s protocol using the TRIzol reagent (Invitrogen, Carlsbad, CA, USA). The concentration of the extracted RNA was determined using a spectrophotometer and then cDNA was constructed with an oligo-$(dT)_{20}$ primer and Superscript III RT (Invitrogen, Carlsbad, CA, USA). PCR amplification was then performed using GOTaq Flexi DNA polymerase (Promega, Madison, WI, USA) and specific primers (Table 1) to amplify the resulting cDNA. The PCR products were separated on a 1% agarose gel electrophoresis system stained with ethidium bromide and the gel was viewed under UV transilluminator 2000 (Bio-Rad).

2.10. Western blot analysis

RIPA buffer containing 50 mM Tris − HCl (pH 7.4), 150 mM NaCl, 1% Nonidet P-40, 0.1 % sodium dodecyl sulfate and a cocktail of protease and phosphatase inhibitors was used to lyse RAW264.7 macrophages and NK-92 cells. The concentrations of proteins were measured using the Pierce BCA Protein Assay kit (Thermo Fisher Scientific). Cell lysates with equal amounts of 30 μg protein were run on an SDS-polyacrylamide gel and therefrom transferred onto a polyvinylidene fluoride (PVDF) membrane. Then, the membrane was incubated with primary antibodies of anti-phospho-NF-κB p65, anti-phospho-JNK, anti-phospho-ERK and anti-phospho-p38. After washing the membrane, it was incubated with HRP-conjugated anti-rabbit antibody for 1 h at 4 °C. The detection of proteins was performed by Pierce ECL Plus Western Blotting Substrate (Thermo Fisher Scientific) which was later visualized using Bio-Rad image analysis system (Bio-Rad Laboratories, Hercules, CA) and finally quantified by Quantity One (version 4.6, Bio-Rad, USA).

2.11. Statistical analyses

Statistical analysis was carried out using SPSS software (version 16; SPSS Inc., Chicago, IL, USA) and all experiments were performed in three independent experiments ($n = 3$). The data are presented as mean ± standard deviation (SD) and significant differences between the test groups were identified by one-way analysis of variance (ANOVA) and Duncan´s multiple-range test. A probability value of $p < 0.05$ was considered to be statistically significant.

3. Results and discussions

3.1. Chemical composition

The yield and proximate chemical composition of polysaccharide from *Ferula gummosa* (FGP) are presented in Table 2. The extraction yield of FGP was 20.3 % which was close to that of the crude polysaccharide we previously obtained from the exudates of *Boswellia carterii* (23.0 %) (Bahramzadeh et al., 2019). The amounts of polysaccharides isolated from plant exudates seem to be widely variable and species-dependent so that on one end of the range we have exudates with low polysaccharide content such as those from *Amygdalus scoparia* (8.021 %) and *Ananas composus* (10.6 %), and on the other end we have polysaccharide-rich exudates such as those from *Launaea acanthodes* (33 %) and *Prunus persica* (45 %) (Molaei & Jahanbin, 2018; Piazza, Bertini, & Milany, 2010; Qian, Cui, Wang, Wang, & Zhou, 2011; Simas-Tosin et al., 2013). In the present study, when the FGP was loaded on to the DEAE Sepharose FF column only a single fraction was obtained meaning the FGP molecules were homogeneous in terms of electric charge distribution (Fig. 1A). The compositional analysis of FGP showed that chains of the extracted polysaccharide were mainly consisted of neutral sugars (90.0 %) and limited amount of uronic acid (4.0

Table 1
Sequences of primers used for rt-PCR.

Gene	Primer sequences (5′ → 3′)
iNOS	(F)CTGCAGCACTTGGATCAGGAACCTG;(R)GGGAGTAGC CTGTGTGCACCTGGAA
IL-1β	(F)ATGGCAACTATTCCAGAACTCAACT;(R)CAGGACAGGTATAGATTCTTTCCTTT
IL-6	(F)TTCCTCTCTGCAAGAGACT;(R)TGTATCTCTCTGAAGGACT
TNF-α	(F)ATGAGCACAGAAAGCATGATC;(R)TACAGGCTTGTCACTCGAATT
IL-12	(F)CCACAAAGGAGGCGAGACTC;(R)CTCTACGAGGAACGCACCTT
β-actin	(F)ATGTGCAAAAAGCTGGCTTTG;(R)ATTTGTGGTGGATGATGGAGG
IF-γ	(F)GATGCTCTTCGACCTCGAAACAGCAT;(R)ATGAAATATACAAGTTATAATCTTGGCTTT
Granzyme-B	(F)AGATCGAAAGTGCGAATCTGA;(R)TTCGTCCATAGGAGACAATGC
Perforin	(F)AGTCCTCCACCTCGTTGTCCGTGA;(R)AAAGTCAGCTCCACTGAAGCTGTG
NKG2D	(F)GACTTCACCAGTTTAAGTAAATC;(R)CTGGGAGATGAGTGAATTTCATA
FasL	(F)CCAGAGAGAGCTCAGATACGTTGAC;(R)ATGTTTCAGCTCTTCCACCTACAGA
β-actin	(F)CATCTCTTGCTCGAAGTCCA;(R)ATCATGTTTGAGACCTTCAACA

Table 2
Yield and chemical composition of FGP from *F. gummosa*.

Sample		
Yield (%)		20.3
Neutral sugars (%)		90.0 ± 0.46
Protein (%)		0.4 ± 0.05
Uronic acid (%)		2.8 ± 0.8
Monosaccharides (%)	Arabinose	11.6 ± 0.64
	Galactose	88.2 ± 0.36
$M_w \times 10^3$ (g/mol)		50.0 ± 0.31
R_g (nm)		105.3 ± 1.94
SV_g (cm^3/g)		58.45

%) (Table 2). The sugar analysis revealed that the FGP was constituted of galactose (88.2 %) and arabinose (11.2 %) units. The presence of arabinogalactans as the major structural unit of polysaccharides has been previously reported in other plants such as *B. carterii*, coffee and *Ixeris polycephala* (Bahramzadeh et al., 2019; Ferreira et al., 2018; Luo et al., 2018).

3.2. Molecular characteristics of FGP

The molecular characteristics of FGP were specified by multi angle laser light scattering technique (MALLS) using a high performance size exclusion column (HPSEC). The refractive index (RI) profile of FGP is represented in Fig. 1C. The FGP molecules were eluted from SEC column between elution times of 36 and 51 min and appeared as a Gaussian-shaped peak with narrow molecular size distribution around the peak maximum which indicated the molecular homogeneity of the polymer. The weight average molecular weight (M_w) and radius of gyration (R_g) of the polysaccharide were 50.0×10^3 g/mol and 105.3 nm, respectively (Table 2). A large deviation exists in the M_w of arabinogalactans extracted from plant exudates; for instance, the M_w measured for arabinogalactan from *A. scoparia* was 4860×10^3 g/mol, but that of *Magnifera indica* was 22×10^3 g/mol (Molaei & Jahanbin, 2018; Nagel, Conrad, Leitenberger, Carle, & Neidhart, 2016).

The specific volume of gyration (SV_g) of the FGP molecules was calculated using R_g and M_w values based on the following equation (You & Lim, 2000) where SV_g, M_w and R_g units are cm^3/g, g/mol and nm, respectively and N is Avogadro's number (6.02×10^{23}/mol):

$$SV_g = 4/3\pi(R_g \times 10^8)^3/(M_w/N) = 2.522\ R_g{}^3/M_w$$

In fact, the SV_g value is the theoretical gyration volume per unit of molar mass and has a reverse relationship to the degree of molecular compactness. The SV_g value of FGP was calculated about 58.45 cm^3/g.

3.3. Methylation and NMR analysis

Methylation analysis was carried out to elucidate the intermolecular linkages of sugar units in the FGP structure. As shown in Fig. 2A and Table 3, five PMAAs derivatives were detected on the GC–MS system among which 1,5,6-tri-*O*-acetyl-2,3,4-tri-*O*-methyl-Gal (Fig. 2C) was the most abundant products revealing 1,6-linked galactopyranose residues formed the backbone of FGP structure. Next to that, a considerably large amount of 1,3,5,6-tetra-*O*-acetyl-2,4-di-*O*-methyl-Gal (Fig. 2D) was found which indicated that FGP structure is highly branched at 1,3,6-linked galactopyranose residues. In addition, the presence of 1,3,5-tri-*O*-acetyl-2,4,6-tri-*O*-methyl-Gal (Fig. 2E) products

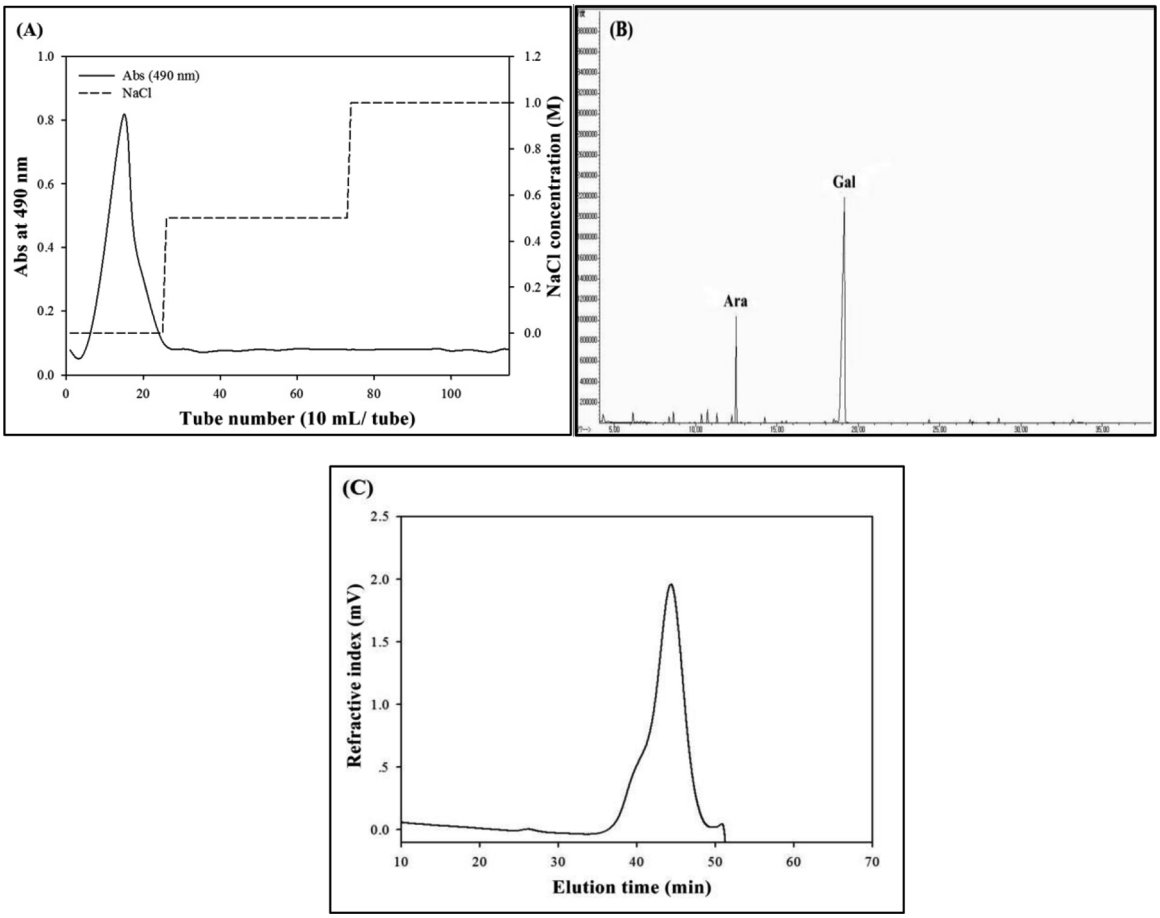

Fig. 1. Elution profile on DEAE Sepharose FF column (A), GC chromatogram of monosaccharides (B) and refractive index profile on a TSK G5000PW column (C) of FGP from *F. gummosa*.

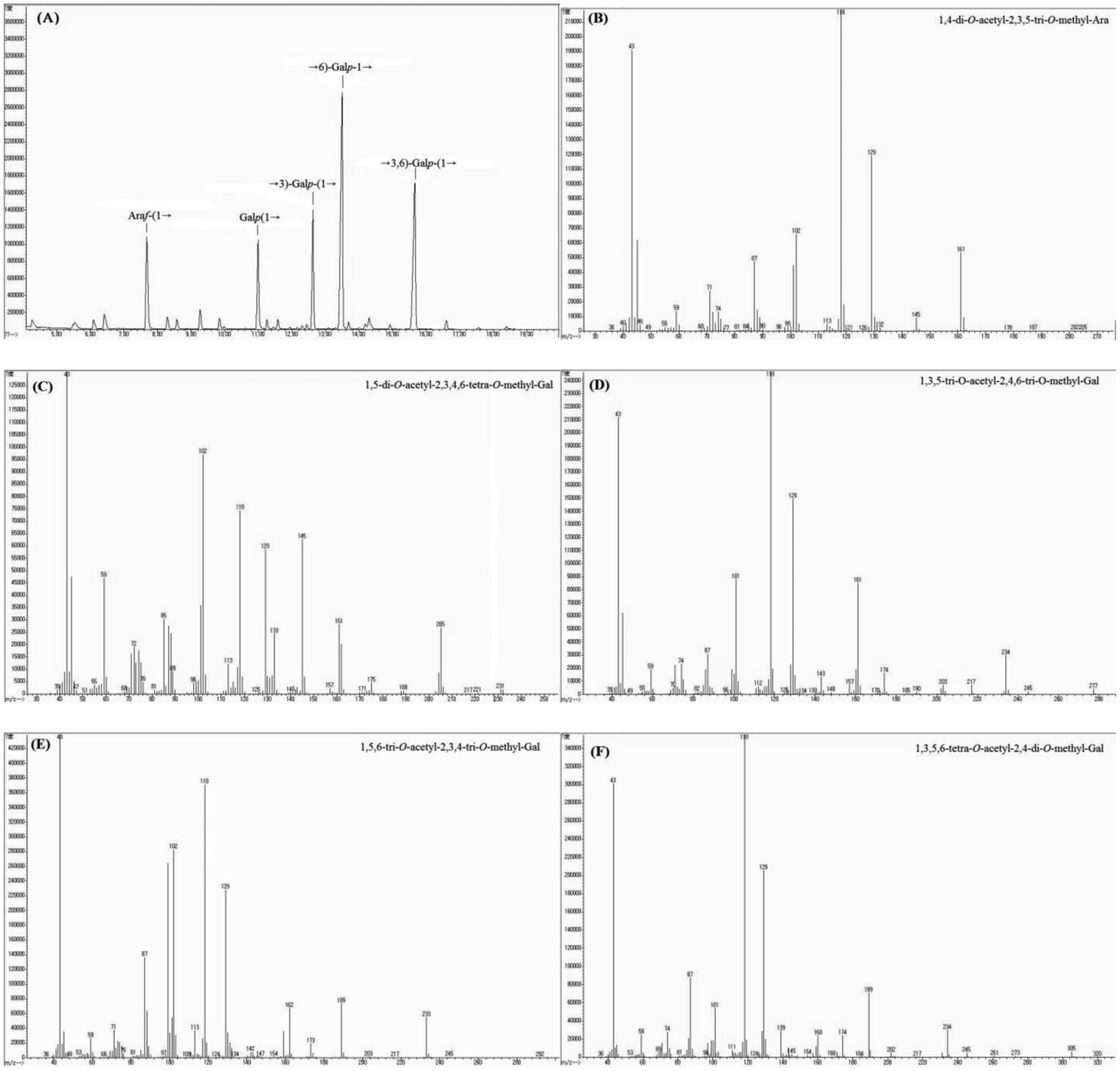

Fig. 2. GC–MS chromatogram (A) of FGP and mass fragments of peaks at 7.68 (B), 10.99 (C), 12.63 (D), 13.50 (E) and 15.66 (F) min.

Table 3
Glycosidic linkage analysis of FGP from *F. gummosa.*

Retention time (min)	Methylation	Glycosidic linkages	Peak ratio (%)
7.68	1,4-di-*O*-acetyl-2,3,5-tri-*O*-methyl-Ara	Ara*f*-(1→	13.3
10.99	1,5-di-*O*-acetyl-2,3,4,6-tetra-*O*-methyl-Gal	Gal*p*(1→	10.9
12.63	1,3,5-tri-*O*-acetyl-2,4,6-tri-*O*-methyl-Gal	→3)-Gal*p*-(1→	13.3
13.50	1,5,6-tri-*O*-acetyl-2,3,4-tri-*O*-methyl-Gal	→6)-Gal*p*-1→	36.6
15.66	1,3,5,6-tetra-*O*-acetyl-2,4-di-*O*-methyl-Gal	→3,6)-Gal*p*-(1→	26.0

showed that some galactose units constitute the side chains of FGP as 1,3-linked galactopyaronse residues. Roughly proportionate to the ratio of branched residues (26.0 %), a total amount of 24.2 % of 1,5-di-*O*-acetyl-2,3,4,6-tetra-*O*-methyl-Gal (Fig. 2F) and 1,4-di-*O*-acetyl-2,3,5-tri-*O*-methyl-Ara (Fig. 2B) products were also identified indicating the presence of galactose and arabinose residues at non-reducing terminals of FGP structure.

In consistent with methylation results, the ^{1}H-NMR spectrum of FGP showed five anomeric proton signals at 5.38, 4.83, 4.70, 4.65 and 4.63 ppm with corresponding ^{13}C signals at 109.50, 103.87, 102.98, 104.12 and 104.22 ppm (Fig. 3A, Table 4). These anomeric signals respectively from downfield to upfield were assigned to α-Ara*f*-(1→, →6)-β-Gal*p*-(1→, β-Gal*p*-(1→, →3)-β-Gal*p*-(1→ and →3,6)-β-Gal*p*-(1→ residues (Tang et al., 2018; Yang, Prasad, & Jiang, 2016; Yao, Yao, Du, Wang, & Ding, 2018; Zhou et al., 2018). The occurrence of two downfield shifts of C-3 to 82.35 and 81.68 ppm indicated the presence of 3-substituted units relating to 1,3-β-Gal*p* and 1,3,6-β-Gal*p* residues (Yang et al., 2016; Zhou et al., 2018). Besides, two more signals shifted

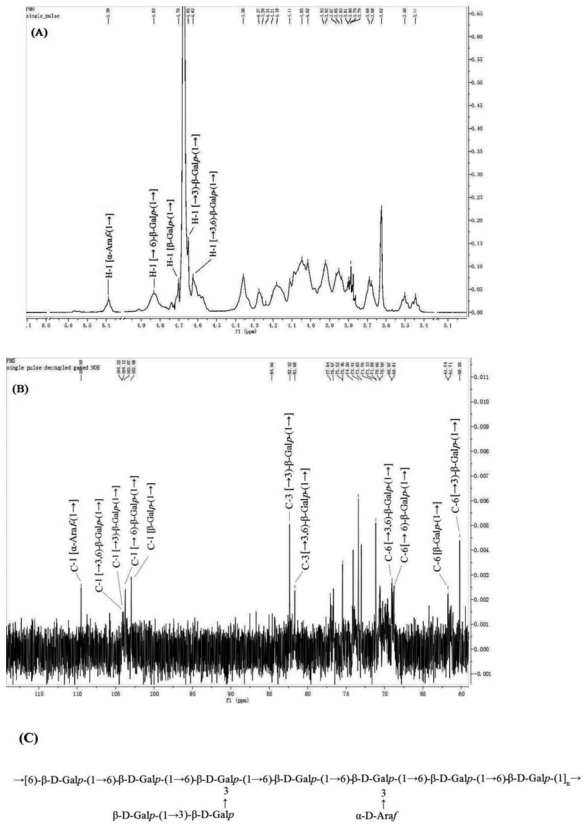

Fig. 3. ^{1}H- (A), ^{13}C-NMR (B) spectra, and putative structure (C) of FGP. NMR spectra were recorded in D_2O at 50 °C.

Table 4
Chemical shift assignments of FGP from *F. gummosa.*

Residues	C-1 H-1	C-2 H-2	C-3 H-3	C-4 H-4	C-5 H-5	C-6 H-6
α-Araf-(1→	109.50	81.70	77.03	84.60	61.74	–
	5.39	4.36	4.18	4.25	3.92	–
β-Galp-(1→	102.98	71.13	74.10	70.66	76.60	61.71
	4.70	3.83	4.02	4.24	4.20	3.50
→3)-β-Galp-(1→	104.12	73.03	82.35	69.08	75.46	60.20
	4.65	3.69	3.80	3.93	3.88	3.44
→6)-β-Galp-(1→	103.87	71.04	73.41	70.60	74.20	69.01
	4.83	3.85	4.05	4.27	4.11	3.78
→3,6)-β-Galp-(1→	104.22	71.57	81.68	69.00	75.50	69.06
	4.63	3.62	3.79	3.90	3.86	3.80

downfield to 69.06 and 69.01 ppm showing the presence of 6-substituted units relating to 1,6-β-Gal*p* and 1,3,6-β-Gal*p* residues (Yang et al., 2016; Zhou et al., 2018). It is noteworthy to mention that although a limited amount of uronic acid was detected in the polysaccharide structure, no distinct signal was observed in the NMR spectra plausibly due to complexity and poor quality of the data. The sheer volume of reports on plant arabinogalactans suggests that predominantly a combination of 3- and 6-linked galactopyranosyls forms their intermolecular structures. Based on the alternating unit, the backbone of the polysaccharide chain of this type of arabinogalactans is either constituted of →3)-β-D-galactopyranosyl-(1→, found in *Lycium barbarum* and *Larix principis-rupprechtii* (Tang et al., 2018; Zhou et al., 2018), or →6)-β-D-galactopyranosyl-(1→ residues, found in *Litchi chinensis* Sonn., *Boswellia carterii* and *Carthamus tinctorius* L. (Bahramzadeh et al., 2019; Yang et al., 2016; Yao et al., 2018) residues. On the basis of these results, the possible structure for FGP and their assumed configurations are shown in Fig. 3C.

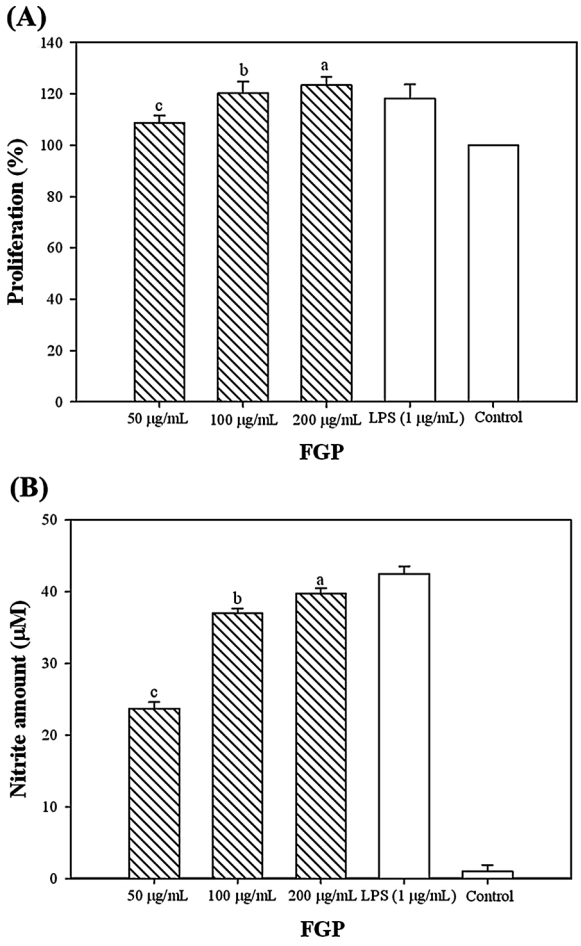

Fig. 4. Proliferation of FGP-stimulated RAW264.7 cells (A) and nitrite amount in the culture medium. The letters a,b,c indicate a significant difference ($p < 0.05$) between the concentrations of the polysaccharides ($p < 0.05$).

3.4. RAW264.7 macrophage proliferation and nitric oxide production

The effect of isolated polysaccharide on the proliferation of RAW264.7 cells was tested over the concentrations ranging from 50 to 200 μg/mL (Fig. 4A). No cytotoxic effect was observed after the addition of polysaccharides into the culture medium of macrophage cells incubated for 18 h. The FGP was not only non-toxic towards RAW264.7 cells but also induced significant proliferation (26 %) at 200 μg/mL ($p < 0.05$). The proliferation of RAW264.7 cells was accompanied with their induction to produce nitric oxide (NO) which was considerably high at 200 μg/mL of FGP releasing 40 μM of nitrite into the culture medium ($p < 0.05$) (Fig. 4B). Indeed, FGP was capable of stimulating RAW264.7 cells to secrete nitrite with comparable magnitude to lipopolysaccharide from *Escherichia coli* (1 ug/mL), although at significantly higher concentration. Regarding the effect of structural properties of polysaccharides on the type of their biological functions, the general notion is that the substitution of functional groups, molecular weight and conformations, drive the overall cell stimulation capacity of a polysaccharide (Ferreira, Passos, Madureira, Vilanova, & Coimbra, 2015). The higher effectiveness of polysaccharides with smaller molecular weights from *Boswellia carterii* (Bahramzadeh et al., 2019) and from *Sargassum angustifolium* (Borazjani, Tabarsa, You, & Rezaei, 2017), larger molecular weights from *Saposhnikovia divaricate* and *Chlorella ellipsoidea* (Dong et al., 2018; Qi & Kim, 2018), higher sulfate groups from *Sargassum angustifolium* and protein-polysaccharide covalent bonding from *Codium fragile* have been previously reported by different studies (Tabarsa et al., 2015). Herein, the type and extent of impact which a polysaccharide molecular weight could have on its cell

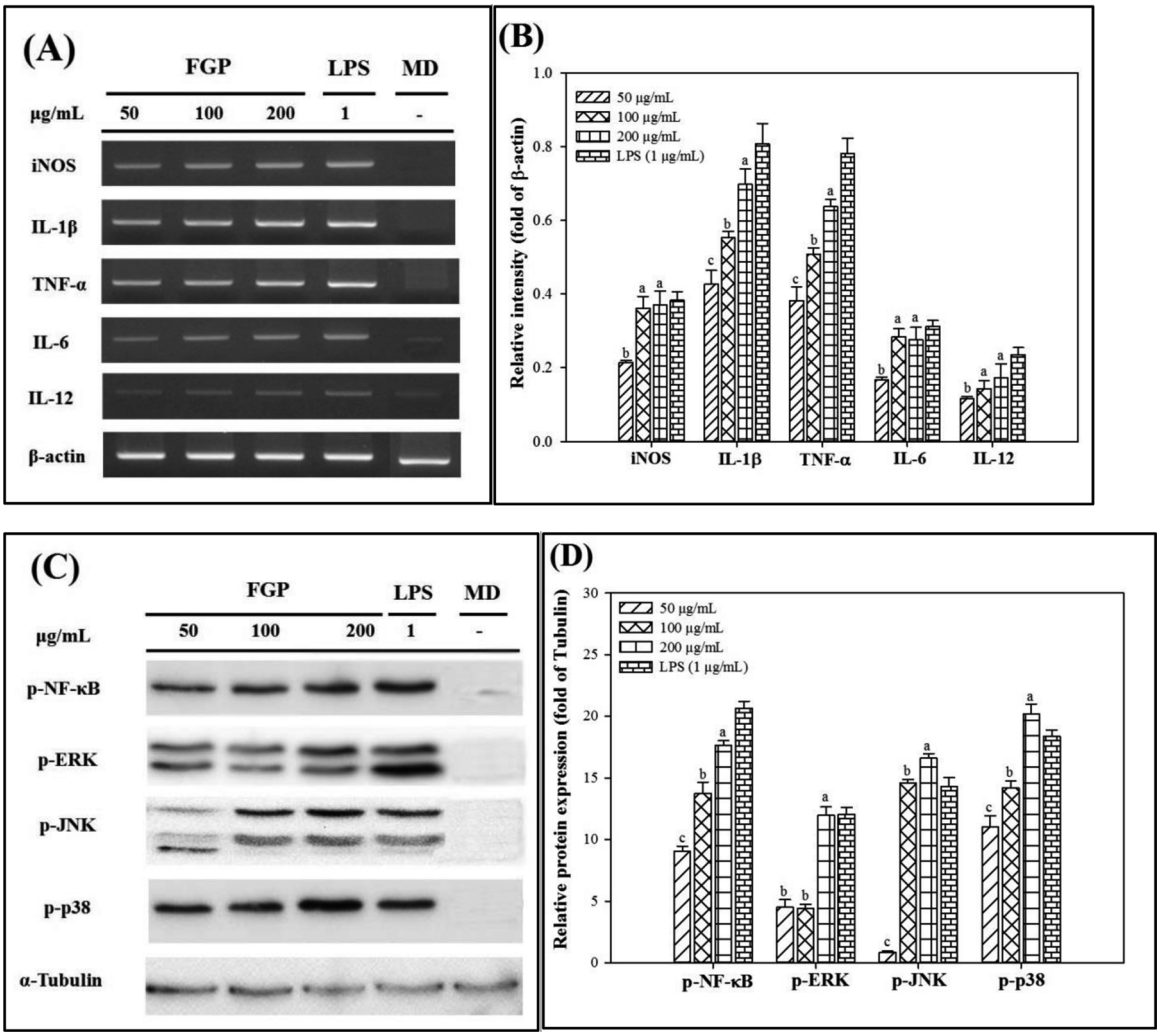

Fig. 5. mRNA expressions of iNOS, IL-1β, TNF-α, IL-6 and IL-12 in FGP-induced RAW264.7 cells (A and B). Levels of p-NF-κB, p-ERK, p-JNK and p-p38 proteins in FGP-induced RAW264.7 cells (C and D). The letters a,b,c indicate a significant difference ($p < 0.05$) between the concentrations of polysaccharides. Both β-actin and α-Tubulin were used as controls. MD represents cells cultured in FGP-free culture medium.

stimulation activity depends on the necessity of being in a certain range of molecular size to allow a polymer approach immune cells and make proper cell-polysaccharide interaction. In case this is not applied to a polysaccharide, the presence of functional groups like sulfate esters or the extended conformation could play a pivotal role and prevail over the hindrance imposed by physical restrictions. Hence, in the current study, the speculation is that the optimum magnitude of molecular weight and conformational extension of FGP led to a noticeable macrophage.

The evaluation of stimulatory effect of FGP on RAW264.7 cells was further explored at the molecular level with the primary aim of looking into the mRNA transcriptions of key proinflammatory mediators. As shown in Fig. 5A and B, the levels of iNOS mRNA, the inducible nitric oxide synthase, was gradually but significantly increased in the stimulated RAW264.7 cells with increased concentrations of FGP ($p < 0.05$) meaning that the enhanced amount of NO in the culture medium was driven by up-regulation of iNOS mRNA expression. Additionally, FGP up-regulated the mRNA expressions of proinflammatory cytokines including IL-1β, TNF-α, IL-6 and IL-12 as suggested by the steady increase of distinct and strong bands of PCR products on the agarose gel (Fig. 5A and B). So far, the results showed that FGP acted as external stimuli of RAW264.7 cells causing significant inflammatory response the exact mechanism of which was thus sought through signaling pathways.

Accordingly, Western blot analysis of the cellular proteins using specific antibodies was explored and the results revealed the presence of high levels of phosphorylated nuclear factor-kappa B (p-NF-κB) (Fig. 5C and D). Basically, NF-κB is an inactive transcription factor, belonging to rapid-acting primary transcription factors, that exists in the cytoplasm of nearly all animal cells where its activity is hindered by a series of inhibitory proteins named iκB. Macrophage cells, once activated, trigger a specific signaling pathway through which NF-κB/ iκB complex undergoes a phosphorylation process and released p-NF-κB protein migrates into the nucleus initiating the mRNA transcription of proinflammatory mediators such as TNF-α and iNOS (Denkers, Butcher, Del Rio, & Kim, 2004). In the current study, as against the untreated cells, the presence of p-NF-κB in FGP-induced RAW264.7 cells suggested the leading role of NF-κB signaling pathway in the activation process. We also looked into the possible occurrence of phosphorylation of JNK, ERK and p38 proteins and results showed positive increase of cellular p-JNK, p-ERK and p-p38 proteins in response to FGP stimulation (Fig. 5C and D). The detection of the three mitogen activated protein kinases (MAPKs) indicated that the stimulation of RAW264.7 cells by FGP was mainly mediated through both MAPKs and NF-κB signaling pathways.

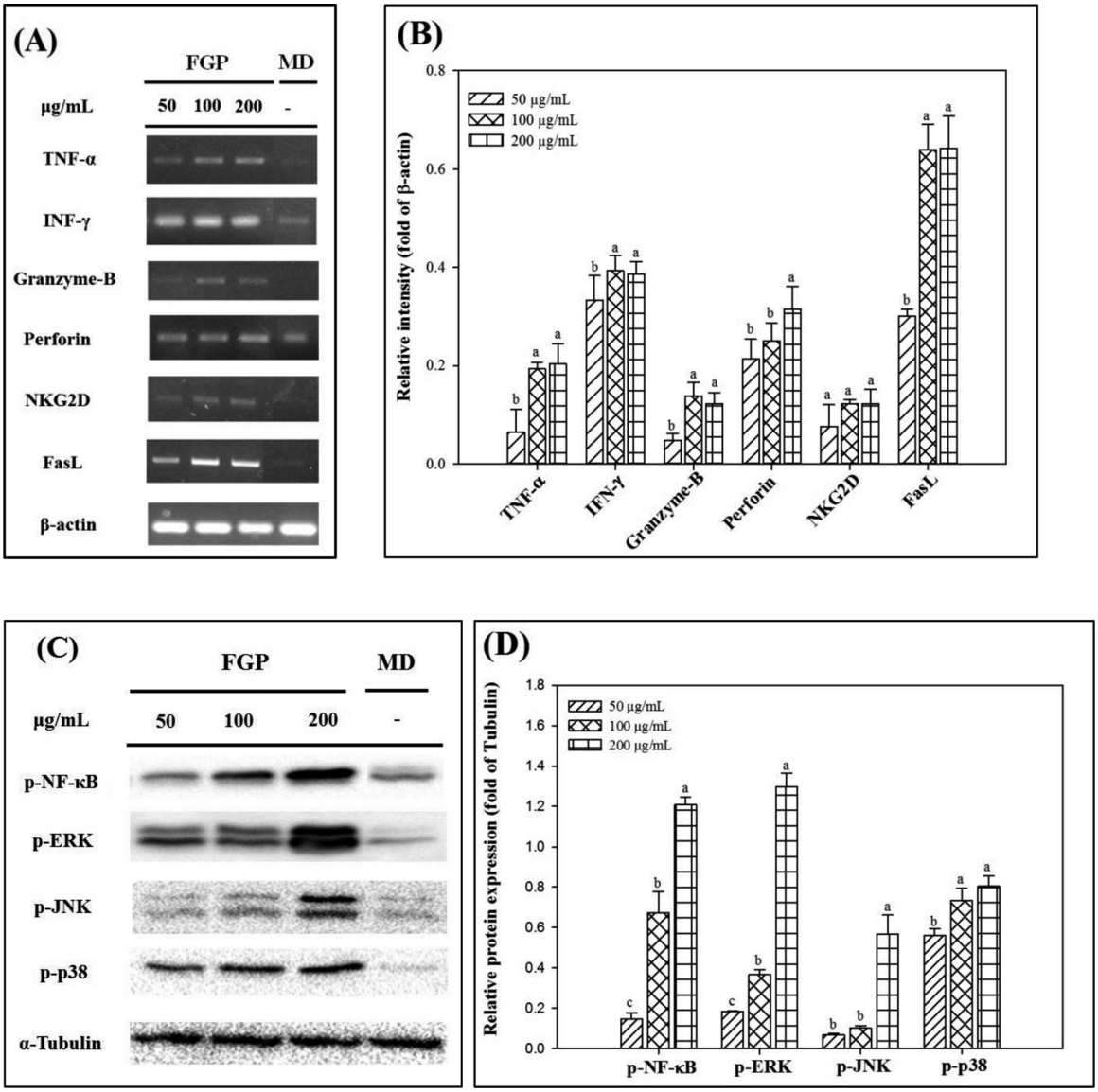

Fig. 6. mRNA expressions of TNF-α, IFN-γ, granzyme-B, perforin, NKG2D and FasL in FGP-induced NK-92 cells (A and B). Levels of p-NF-κB, p-ERK, p-JNK and p-p38 proteins in FGP-induced NK-92 cells (C and D). The letters a,b,c indicate a significant difference ($p < 0.05$) between the concentrations of polysaccharides. Both β-actin and α-Tubulin were used as controls. MD represents cells cultured in FGP-free culture medium.

3.5. NK-92 activation by FGP

Natural killer (NK) cells are in fact lymphocytes originating from a common progenitor as T and B cells. However, as a member of the innate immune system, NK cells are capable of responding quickly to a broad spectrum of pathological challenges. In the present investigation, we examined the possibility of NK-92 cell activation by FGP using mRNA expressions of inflammatory cytokines including TNF-α, IFN-γ, granzyme-B, perforin, NKG2D and FasL. As illustrated in Fig. 6A and B, FGP induced a significant up-regulation in the mRNA expressions of TNF-α and IFN-γ cytokines over the concentration range of 50–200 μg/mL. Similarly, compared with untreated NK-92 cells, the addition of FGP into the culture medium up-regulated the mRNA expressions of granzyme-B and perforin. A dose-dependent increase was also observed in the mRNA levels of apoptosis-inducing ligand (FasL) and activating receptor NKG2D after FGP treatment. NK cells actively engage in the surveillance and defense mechanism of immune system against virally infected cells and tumor cells, without any priming, via either release of cytokines or direct cytotoxicity (Smyth et al., 2000; Trinchieri, 1989). Activated NK cells synthesize and secrete IFN-γ and TNF-α into the surrounding area upon which a series of profoundly effective inflammatory responses initiates, leading to activation of macrophage and dendritic cells, acceleration of immune cell recruitment into the affected site and direct antiviral activities (Paolini, Bernardini, Molfetta, & Santoni, 2015). Direct defense mechanism begins when NK cells approach the target cells and their newly formed cytoplasmic granules become first disintegrated and then released perforins bind to the membrane of the target creating an aqueous channel for granzymes to enter the cell and induce apoptosis (Smyth et al., 2005).

We then searched for possible signaling pathways playing key roles in the activation of NK-92 cells by FGP. The incubation of NK-92 cells for 24 h with FGP resulted in steady increasing levels of p-NF-κB in comparison with untreated cells (Fig. 6C and D). Likewise, the amount of phosphorylated MAPK proteins including p-ERK, p-JNK and p-p38 elevated in FGP-induced NK-92 cells (Fig. 6C and D). The overall findings of these assays suggested that FGP is also capable of inducing NK-92 cells via both NF-κB and MAPKs signaling pathways.

4. Conclusions

A high yielded polysaccharide was obtained from *F. gummosa* (FGP) possessing a homogenous and uniform molecular weight distribution. The FGP was found to be an arabinogalactan with a backbone formed of →6)-β-Gal*p*-1→, β-Gal*p*-(1→3)-β-Gal*p*-(1→ and α-Ara*f*-(1→ as well as →3,6)-β-Gal*p*-1→ as branching points. FGP activated immune cells to exert proinflammatory response expressing a wide range of inflammatory mediators including NO, TNF-α, IL-1β, IL-6 and IL-12 in RAW264.7 cells and TNF-α, IFN-γ, granzyme-B, perforin, NKG2D and FasL in NK-92 cells. The stimulation of RAW264.7 and NK-92 cells took place via the activation of NF-κB and MAPKs signaling pathways. Overall, these results indicated the potency of polysaccharides from the exudates of *F. gummosa* to boost human immune system.

CRediT authorship contribution statement

Mehdi Tabarsa: Conceptualization, Methodology, Supervision. **Elham Hashem Dabaghian:** Methodology, Investigation. **SangGuan You:** Conceptualization, Methodology, Supervision. **Khamphone Yelithao:** Methodology, Data curation, Investigation. **Subramanian Palanisamy:** Methodology, Software. **Narayanasamy Marimuthu Prabhu:** Methodology, Writing - review & editing. **Changsheng Li:** Methodology, Investigation.

Acknowledgement

We are grateful for the support provided by Tarbiat Modares University (IG-39807) and Basic Science Research Program through the National Research Foundation of Korea (NRF) funded by the Ministry of Education (No. 2018R1A6A1A03023584).

References

Bahramzadeh, S., Tabarsa, M., You, S., Yelithao, K., Klochkov, V., & Ilfat, R. (2019). An arabinogalactan isolated from *Boswellia carterii*: Purification, structural elucidation and macrophage stimulation via NF-κB and MAPK pathways. *Journal of Functional Foods, 52*, 450–458.

Bao, X., Yuan, H., Wang, C., Liu, J., & Lan, M. (2013). Antitumor and immunomodulatory activities of a polysaccharide from *Artemisia argyi*. *Carbohydrate Polymers, 98*(1), 1236–1243.

Borazjani, N. J., Tabarsa, M., You, S., & Rezaei, M. (2017). Effects of extraction methods on molecular characteristics, antioxidant properties and immunomodulation of alginates from *Sargassum angustifolium*. *International Journal of Biological Macromolecules, 101*, 703–711.

Canton, J., Neculai, D., & Grinstein, S. (2013). Scavenger receptors in homeostasis and immunity. *Nature Reviews Immunology, 13*(9), 621.

Ciucanu, I., & Kerek, F. (1984). A simple and rapid method for the permethylation of carbohydrates. *Carbohydrate Research, 131*, 209–217.

Denkers, E. Y., Butcher, B. A., Del Rio, L., & Kim, L. (2004). Manipulation of mitogen--activated protein kinase/nuclear NF-κB signaling cascades during intracellular *Toxoplasma gondii* infection. *Immunological Reviews, 201*(1), 191–205.

Dong, C. X., Liu, L., Wang, C. Y., Fu, Z., Zhang, Y., Hou, X., & Yao, Z. (2018). Structural characterization of polysaccharides from *Saposhnikovia divaricata* and their antagonistic effects against the immunosuppression by the culture supernatants of melanoma cells on RAW264.7 macrophages. *International Journal of Biological Macromolecules, 113*, 748–756.

Dubois, M., Gilles, K. A., Hamilton, J. K., Rebers, P. T., & Smith, F. (1956). Colorimetric method for determination of sugars and related substances. *Analytical Chemistry, 28*(3), 350–356.

Feng, Y. Y., Ji, H. Y., Dong, X. D., Yu, J., & Liu, A. J. (2019). Polysaccharide extracted from *Atractylodes macrocephala* Koidz (PAMK) induce apoptosis in transplanted H22 cells in mice. *International Journal of Biological Macromolecules, 137*, 604–611.

Ferreira, S. S., Passos, C. P., Cepeda, M. R., Lopes, G. R., Teixeira-Coelho, M., Madureira, P., & Coimbra, M. A. (2018). Structural polymeric features that contribute to in vitro immunostimulatory activity of instant coffee. *Food Chemistry, 242*, 548–554.

Ferreira, S. S., Passos, C. P., Madureira, P., Vilanova, M., & Coimbra, M. A. (2015). Structure–function relationships of immuno-stimulatory polysaccharides: A review. *Carbohydrate Polymers, 132*, 378–396.

Filisetti-Cozzi, T. M. C. C., & Carpita, N. C. (1991). Measurement of uronic acids without interference from neutral sugars. *Analytical Biochemistry, 197*, 157–162.

Green, L. C., Wanger, D. A., Glogowski, J., Skipper, P. L., Wishnok, J. S., & Tannenbaum, S. R. (1982). Analysis of nitrate, nitrite, and [15N] nitrate in biological fluids. *Analytical Biochemistry, 126*, 131–136.

Khan, T., Date, A., Chawda, H., & Patel, K. (2019). Polysaccharides as potential anticancer agents—A review of their progress. *Carbohydrate Polymers, 210*, 412–428.

Liang, S., Li, X., Ma, X., Li, A., Wang, Y., Reaney, M. J., & Shim, Y. Y. (2019). A flaxseed heteropolysaccharide stimulates immune responses and inhibits hepatitis B virus. *International Journal of Biological Macromolecules, 136*, 230–240.

Liu, J., Willför, S., & Xu, C. (2015). A review of bioactive plant polysaccharides: Biological activities, functionalization, and biomedical applications. *Bioactive Carbohydrates and Dietary Fibre, 5*(1), 31–61.

Lowry, O. H., Rosebrough, N. J., Farr, A. L., & Randall, R. J. (1951). Protein measurement with the Folin phenol reagent. *Journal of Biological Chemistry, 193*, 265e–275.

Luo, B., Dong, L. M., Xu, Q. L., Zhang, Q., Liu, W. B., Wei, X. Y., & Tan, J. W. (2018). Characterization and immunological activity of polysaccharides from *Ixeris polycephala*. *International Journal of Biological Macromolecules, 113*, 804–812.

Luo, J., Qi, J., Wang, W., Luo, Z., Liu, L., Zhang, G., ... Peng, X. (2019). Antiobesity effect of flaxseed polysaccharide via inducing satiety due to leptin resistance removal and promoting lipid metabolism through the AMPK signaling pathway. *Journal of Agricultural and Food Chemistry, 67*, 7040–7049.

Molaei, H., & Jahanbin, K. (2018). Structural features of a new water-soluble polysaccharide from the gum exudates of *Amygdalus scoparia* Spach (Zedo gum). *Carbohydrate Polymers, 182*, 98–105.

Muschin, T., Budragchaa, D., Kanamoto, T., Nakashima, H., Ichiyama, K., Yamamoto, N., ... Yoshida, T. (2016). Chemically sulfated natural galactomannans with specific antiviral and anticoagulant activities. *International Journal of Biological Macromolecules, 89*, 415–420.

Nagel, A., Conrad, J., Leitenberger, M., Carle, R., & Neidhart, S. (2016). Structural studies of the arabinogalactans in *Mangifera indica* L. fruit exudate. *Food Hydrocolloids, 61*, 555–566.

Paolini, R., Bernardini, G., Molfetta, R., & Santoni, A. (2015). NK cells and interferons. *Cytokine & Growth Factor Reviews, 26*(2), 113–120.

Piazza, L., Bertini, S., & Milany, J. (2010). Extraction and structural characterization of the polysaccharide fraction of *Launaea acanthodes* gum. *Carbohydrate Polymers, 79*(2), 449–454.

Qi, J., & Kim, S. M. (2018). Effects of the molecular weight and protein and sulfate content of *Chlorella ellipsoidea* polysaccharides on their immunomodulatory activity. *International Journal of Biological Macromolecules, 107*, 70–77.

Qian, H. F., Cui, S. W., Wang, Q., Wang, C., & Zhou, H. M. (2011). Fractionation and physicochemical characterization of peach gum polysaccharides. *Food Hydrocolloids, 25*(5), 1285–1290.

Salehi, M., Naghavi, M. R., & Bahmankar, M. (2019). A review of Ferula species: Biochemical characteristics, pharmaceutical and industrial applications, and suggestions for biotechnologists. *Industrial Crops and Products, 139*, 111511.

Simas-Tosin, F. F., de Souza, L. M., Wagner, R., Pereira, G. C., Barraza, R. R., Wendel, C. F., & Gorin, P. A. (2013). Structural characterization of a glucuronoarabinoxylan from pineapple (*Ananas comosus* (L.) Merrill) gum exudate. *Carbohydrate Polymers, 94*(1), 704–711.

Singh, S., Singh, G., & Arya, S. K. (2018). Mannans: An overview of properties and application in food products. *International Journal of Biological Macromolecules, 119*, 79–95.

Smyth, M. J., Cretney, E., Kelly, J. M., Westwood, J. A., Street, S. E., Yagita, H., ... Hayakawa, Y. (2005). Activation of NK cell cytotoxicity. *Molecular Immunology, 42*(4), 501–510.

Smyth, M. J., Thia, K. Y., Street, S. E., Cretney, E., Trapani, J. A., Taniguchi, M., ... Godfrey, D. I. (2000). Differential tumor surveillance by natural killer (NK) and NKT cells. *The Journal of Experimental Medicine, 191*(4), 661–668.

Soltani, S., Amin, G. R., Salehi-Sourmaghi, M. H., Schneider, B., Lorenz, S., & Iranshahi, M. (2018). Sulfur-containing compounds from the roots of *Ferula latisecta* and their cytotoxic activities. *Fitoterapia, 124*, 108–112.

Song, D. H., & Lee, J. O. (2012). Sensing of microbial molecular patterns by Toll-like receptors. *Immunological Reviews, 250*(1), 216–229.

Tabarsa, M., Park, G. M., Shin, I. S., Lee, E., Kim, J. K., & You, S. (2015). Structure-activity relationships of sulfated glycoproteins from *Codium fragile* on nitric oxide releasing capacity from RAW264. 7 cells. *Marine Biotechnology, 17*(3), 266–276.

Tang, S., Jiang, M., Huang, C., Lai, C., Fan, Y., & Yong, Q. (2018). Characterization of arabinogalactans from *Larix principis-rupprechtii* and their effects on NO production by macrophages. *Carbohydrate Polymers, 200*, 408–415.

Trinchieri, G. (1989). Biology of natural killer cells. *Advances in immunology, 47*, 187–376 Academic Press.

Tripathi, P., Tripathi, P., Kashyap, L., & Singh, V. (2007). The role of nitric oxide in inflammatory reactions. *FEMS Immunology & Medical Microbiology, 51*(3), 443–452.

Xiao, Y., Chen, L., Fan, Y., Yan, P., Li, S., & Zhou, X. (2019). The effect of boletus polysaccharides on diabetic hepatopathy in rats. *Chemico-Biological Interactions, 308*, 61–69.

Yang, B., Prasad, K. N., & Jiang, Y. (2016). Structure identification of a polysaccharide purified from litchi (*Litchi chinensis* Sonn.) pulp. *Carbohydrate Polymers, 137*, 570–575.

Yao, Y., Yao, J., Du, Z., Wang, P., & Ding, K. (2018). Structural elucidation and immune-enhancing activity of an arabinogalactan from flowers of *Carthamus tinctorius* L. *Carbohydrate Polymers, 202*, 134–142.

You, S. G., & Lim, S. T. (2000). Molecular characterization of corn starch using an aqueous HPSEC-MALLS-RI system under various dissolution and analytical conditions. *Cereal Chemistry, 77*, 303–308.

Zhao, B., Lian, J., Wang, D., Li, Q., Feng, S., Li, J., & Zhang, A. (2019). Evaluation of aqueous extracts of *Cistanche deserticola* as a polysaccharide adjuvant for seasonal influenza vaccine in young adult mice. *Immunology Letters, 213*, 1–8.

Zhou, L., Liao, W., Chen, X., Yue, H., Li, S., & Ding, K. (2018). An arabinogalactan from fruits of *Lycium barbarum* L. inhibits production and aggregation of Aβ42. *Carbohydrate Polymers, 195*, 643–651.

Zhou, Y., Xin, F., Zhang, G., Qu, H., Yang, D., & Han, X. (2017). Recent advances on bioactive constituents in Ferula. *Drug Development Research, 78*, 321–331.